Effect of processing conditions on the properties of high molecular weight conductive polyaniline fiber

ARTICLE *in* JOURNAL OF POLYMER SCIENCE PART B POLYMER PHYSICS · JANUARY 2000

Impact Factor: 3.83 · DOI: 10.1002/(SICI)1099-0488(20000101)38:1<194::AID-POLB22>3.0.CO;2-H

Effect of Processing Conditions on the Properties of High Molecular Weight Conductive Polyaniline Fiber

HSING-LIN WANG,[1] ROBERT J. ROMERO,[1] BENJAMIN R. MATTES,[1] YUNTIAN ZHU,[2] MICHAEL J. WINOKUR[3]

[1] Chemical Science and Technology Division, MS J-585, Los Alamos National Laboratory, Los Alamos, New Mexico 87545

[2] Material Science and Technology Division, MS G-755, Los Alamos National Laboratory, Los Alamos, New Mexico 87545

[3] Department of Physics, University of Wisconsin, 1150 University Avenue Madison, Wisconsin 53706

Received 11 May 1999; revised 22 September 1999; accepted 4 October 1999

ABSTRACT: Polyaniline–emeraldine base (EB) fiber with excellent mechanical and electrical properties have been spun from highly concentrated (20% w/w), EB/*N*-methyl-2-pyrrolidinone (NMP)/2-methylaziridine (2 MA) solution. These solutions had gelation times, which varied from hours to days depending on the molar ratio of 2 MA to EB tetramer repeating unit in the *N*-methyl-2-pyrrolidinone (NMP) solvent. To better compare the mechanical and electrical properties, dense films were also prepared by thermal evaporation of less concentrated solution (1% w/w). Both fibers and films were amenable to thermal stretching with maximum draw ratios of 4 : 1 and these stretched samples exhibited the greatest tensile strength overall. Wide-angle X-ray diffraction (WAXD) of as-spun and 4-times stretched fiber showed a completely amorphous structure. Fiber subjected to heat treatment at 250 °C under N_2 flux for 2 h displayed further improvements in mechanical properties because of crosslinking between the polymer chains. Fibers and films were later doped by immersion in a variety of aqueous acid solutions. Room temperature DC conductivities for the doped samples ranged from 6 $\times 10^{-4}$ to 45 S/cm depending on the specific choice of acid. Scanning electron microscopy of fiber samples shows the presence of macrovoid formation during fiber spinning. Continued refinement of the processing parameters and fiber post-treatment, to enhance chain alignment and increase fiber density, will likely lead to additional improvements in the fiber mechanical and electrical properties. Characterization of emeraldine base (EB) powder, solution, films, and fibers by UV-Vis, DSC, TGA, and WAXD were also performed. J Polym Sci B: Polym Phys 38: 194–204, 2000
Keywords: polyaniline; fiber; processing; mechanical; conductivity

INTRODUCTION

Polyaniline has attracted research interests because of its potential for applications such as light-emitting diodes (LED),[1] actuators,[2] and gas-separation membranes.[3] Among the many potential applications of polyaniline, there is a growing interest in developing highly conductive polyaniline fibers for antistatic purposes because of its low cost and environmental stability. Processing of these materials is still a major limitation because polyaniline, in its base form, is soluble in only a handful of solvents. Moreover, these polyaniline–emeraldine base (EB) solutions have a strong propensity to quickly gel even at dilute concentrations (<5% w/w). This undesirable prop-

Correspondence to: H.-L. Wang (E-mail: hwang@lanl.gov)

Journal of Polymer Science: Part B: Polymer Physics, Vol. 38, 194–204 (2000)

erty becomes even more apparent at the concentrations required for optimal solid fiber spinning (>20% w/w). Gelation times are also a function of the polymer chain length so that increasing the average EB molecular weight further diminishes the solution gelation times.[4] At present, we are unaware of any prior work reporting the preparation of stable 20% w/w high molecular weight (HMW) EB solution in a single solvent system. Processing to form fibers or films has been extensively investigated. MacDiarmid et al. first reported oriented polyaniline–emeraldine base films and fibers in 1991. These fibers were made from concentrated (20% w/w) low molecular weight EB (synthesized at 0 °C) solution and the mechanical strength of these 3–4 times stretched fibers was 366 MPa.[5,6] Although these fibers exhibit only modest properties, in comparison with traditional high-strength fibers, the work of MacDiarmid et al. demonstrated that fiber spinning from concentrated EB solutions is possible. Rapid gelation of these concentrated polyaniline EB solutions was also observed.[4] To partially circumvent this problem,[7,8] Hsu et al. either employed amines such as pyrrolidine directly as solvents or added to NMP as a cosolvent, thereby retarding gelation times and allowing for fiber spinning on a meaningful scale. Subsequent studies by Han et al. revealed aging phenomenon in these amine solutions because of concurrent reduction and nucleophilic substitution of H-atom on the semiquinone ring with pyrrolidine molecule. This aging process could be detected as early as 10 min after the EB/pyrrolidine solutions were prepared.[9] Gregory et al. have obtained spun fiber from low molecular weight (17% w/w) EB solution using solvents such as dimethylpropylene urea (DMPU),[10] and they have recently employed a new approach to spin fiber from a highly concentrated leucoemeraldine base solution.[11] Other groups have spun polyaniline and poly(o-toluidine) fibers from acid doped polymer solution employing very strong sulfuric acid[12] or toxic m-cresol[13] as solvents.

In this article, we report the fabrication of fibers from highly concentrated (>20% w/w) high molecular weight (HMW) EB solutions, which are stabilized through addition of small amounts of secondary amine additives, for example, 2-methylaziridine (2 MA), into the EB/NMP solution.[14] These studies also reveal how processing conditions impact the final fiber properties. Optimization of fiber spinning involves many system parameters such as the composition of the "dope" (final solution that was used for spinning fiber), configuration of the spinneret tip, selection and composition of the coagulation bath, extrusion rate, and fiber uptake velocity. We have also studied the effect of post treatment on the mechanical properties of the fiber. Improvement in the tensile strength, Young's modulus and, after doping, in the electrical conductivity of these fibers was consistently achieved by a combination of thermal annealing, which leads to appreciable crosslinking between chains, and uniaxial stretching which induces partial chain alignment.

EXPERIMENTAL

Materials and Instrumentation

Aniline (99% Aldrich) was distilled under vacuum and stored under nitrogen prior to use. *n*-Methyl-2-pyrrolidinone, 2-methylaziridine, ammonium persulfate, were purchased from Aldrich and were used as received. Synthesis of HMW polyaniline, emeraldine base powder was carried out at −45 °C and the details were reported elsewhere.[14]

Standard 4-probe conductivity measurements were made with a Hewlett-Packard model 3478A digital multimeter to measure conductivity of films and fibers. X-ray scattering profiles were recorded using a customized X-ray powder diffractometer. The X-ray source was a 15 kW rotating anode generator (Enraf–Nonius GX-21) fitted with a copper target $\lambda_{\kappa\alpha} = 1.542$, an elastically bent focusing LiF crystal monochrometer and a 120°2ϑ position sensitive detector (Inel Model CPS-120). The cross-sectional area of the X-ray beam incident at the sample was typically 0.5 × 4.0 mm^2. Helium-filled beam paths were used to minimize absorption and air scatter. In some instances, radial ϑ–2ϑ scans were performed with the samples mounted within the Eulerian cradle and the various polymer fibers maintained in a transmission geometry. By repositioning the sample, scattering data in directions both parallel and perpendicular to the draw direction could be acquired. Differential scanning calorimetry and thermal gravimetric analysis measurements were made with a Perkin–Elmer 7 series thermal analysis system at a heating rate of 5 °C/min. UV-Vis spectra of polymer solution were obtained using the Perkin–Elmer λ9 UV-Vis-NIR spectrometer. Molecular weight measurements were performed by means of a Waters gel permeation chromato-

graph (GPC) on 0.1% (w/w) solutions of EB in NMP at room temperature with an ultrastyragel linear column with a UV detector monitoring 320 nm transmitted light. These polyaniline samples were of high molecular weight, $M_w > 135{,}000$. This molecular weight is significantly higher than that of polyaniline conventionally synthesized at 0 °C without LiCl added to depress the freezing point of water of the reaction mixture as frequently cited in the literature.

Preparation of Concentrated (20.1% w/w) EB Solution

Preparation of the concentrated HMW 20.10% w/w EB solution: 31.32 g of *n*-methyl-2-pyrrolidinone (NMP) was mixed with 4.879 g of 90% 2-methylaziridine. This solution was then placed in a 60 mL glass jar with a screw cap and annealed in a 60 °C oven for about 1 h. Afterwards, 9.109 g of the HMW EB was added to this solution mixture in 30 s. After a few minutes of vigorous stirring the solution mixture appeared to have an almost pastelike consistency. To obtain a homogeneous, particle-free polymer solution, the glass jar was recapped and placed in a 100 °C oven for ~ 30 min. At 10 min intervals the glass jar was removed from the oven and vigorously stirred.

Method of Fiber Extrusion

Once the highly concentrated EB solution was prepared, it was transferred to a hydraulic stainless steel cylinder and cooled to room temperature (25 °C). A gear pump motor assisted by nitrogen gas in the fore-line at 100 psi was used to drive the EB fluid through 3/8′ stainless steel tubing, and then through a single-hole spinneret tip with a 500 μ inner diameter. The polymer solution was extruded through a 2.5 cm air gap into a water coagulation bath (15 °C). The take up speed was set to ~ 6 meters per minute. The nascent fiber was continuously wound onto a series of two water bath godets maintained at 15 °C. Typically, the EB fiber was immersed in a 10-gallon water tank after spinning to extract the NMP solvent and 2-methylaziridine additive. The water in this bath was changed on a daily basis for over a week until the solvent was thoroughly removed. For fibers requiring thermal uniaxial stretching, the fiber was removed from the bath in under 24 h. In this case residual solvent (NMP) is necessary to plasticize the fiber, thereby enabling the fiber to be thermally drawn as described in the following paragraph.

As-spun polyaniline fiber from the EB/NMP/2 MA solution was removed from the water bath and allowed to dry in air for 30 min. A heated copper rod was wrapped with a piece of Teflon sheet and set to 120 °C by means of a Variac temperature controller. Fibers and films were stretched across this assembly while placed under uniaxial tension. Draw ratios for the fibers (and films) were approximately 3–5 times the original length.

Preparation of EB Dense Films

Free-standing EB films were prepared by methods similar to those reported earlier.[15] Thermally annealed dense films were prepared from 1% w/w of EB/NMP/2 MA solution. As a representative procedure, 306 mg of EB powder was added to 30 g of NMP and 102 mg of 2 MA solution mixture. The resulting solution mixture was stirred using a magnetic bar for at least 1 h, and was then put into a 60 °C oven until the homogeneous solution was formed. The solution was poured onto a Teflon template with a 4′ × 2′ cavity. The template was later transferred into a 60 °C air oven where it was left overnight. This allowed the solvent mixture to evaporate until the film became visually dry. Afterwards the film was peeled off from the Teflon template. PANI films prepared by this method contained ~ 16% of residual solvent NMP and this film is reported to have a glass-transition temperature of ~ 105 °C.[16] The remaining NMP molecules are more tightly bonded to the EB chains through H-bonding interaction,[17] which serves to plasticize the film. These films can also be thermally stretched at 105 °C to over 4 times the original length.

Mechanical Testing

All tensile studies were performed in air. Individual fibers were glued at the ends onto 600-grid sandpaper mounts, which gave fiber gauge lengths of 10 mm. Mounted fibers were mechanically secured into an alignment jig, which was then attached to the grips of a microtensile test machine (Micropull Science, Thousand Oaks, CA). The micropull configuration consisted of a load cell, a hydraulically driven stepper motor, and a linear voltage displacement transducer (LVDT) to measure displacement. Fibers were loaded in tension at a constant displacement rate

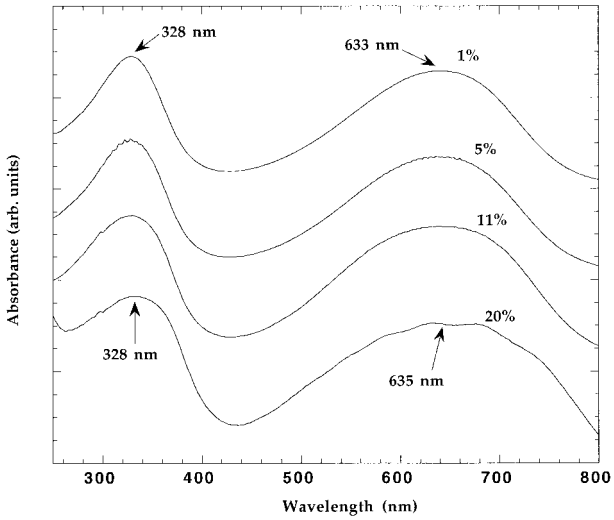

Figure 1. UV-Vis of EB/NMP/2 MA solutions with various concentration.

of 0.3 mm/min until fracture occurred. Load-displacement curves were measured using a personal computer and vendor-provided software. Peak load and average cross-sectional area values were used to calculate the fiber strength. Since initial cross-sectional area and initial gauge length values were used to calculate the stress-strain curve, the strength and strain obtained from the stress–strain curve are engineering stress and strain. Mechanical testing of the thermally cured dense films was also carried out in a similar manner with the same instrument. Typically three tests were performed on each fiber or film sample lot and the reported values in this paper are the average of these three trials.

RESULTS AND DISCUSSION

Polyaniline–Emeraldine Base, EB Solution Properties

Figure 1 displays characteristic UV-Vis spectra from EB/NMP/2 MA solutions with increasing EB concentration (1–20% w/w) and a constant gel-inhibitor (GI) 2 MA/EB molar ratio of 2.5. These spectra are similar to other EB solution spectra without GI and, since these absorption spectra are essentially independent of EB concentration, indicate that the EB remains in its original oxidation state. If reduction of the EB by the GI were to have occurred, the UV-Vis spectrum of the resulting EB would yield just a single absorption peak at 330 nm. The addition of GI also does not impact the bulk electrical transport properties. Thermally cured dense films prepared from the above solutions could be doped by aqueous 1*M* HCl (over 48 h) to the conductive emeraldine salt with conductivities ranging from 1–5 S/cm (these films were subjected to dynamic pumping for 72 h before conductivity measurements to remove water moisture). This was comparable to the measured conductivities of doped EB films obtained without the addition of 2 MA. Gelation times for the 20% w/w EB/NMP/2 MA solution, subsequently used for fiber spinning, at 25 °C exceeded 20 h with a solution viscosity of $\sim$ 3000 cp.[18] When preparing these concentrated EB solutions the exact 2 MA/EB molar ratio was dependent on the specific EB molecular weight. Furthermore, addition of GI to the EB solution did not sacrifice the physical strength of the resulting as-spun fiber.

Effect of Thermal Stretching on the Mechanical Properties of EB Fibers

Averaged stress–strain curves for as-spun and 4-times stretched fibers are shown in Figure 2. Clearly the 4-times stretched fiber exhibits a much higher Young's modulus (1.85 GPa) than that of as-spun fiber (0.54 GPa) where the Young's modulus was defined as the slope within the region of elastic deformation in the stress-strain curve. The yield strength for 4-times stretched fiber, $\sigma_{0.2}$, defined as the stress at 0.2% permanent strain (see Fig. 2), is 50 MPa, as compared to 12 MPa for as-spun fiber. The failure strength, σ_f, is 63 MPa for the 4-times stretched fiber, which is approximately 4-times greater than the 15 MPa failure strength of the as-spun

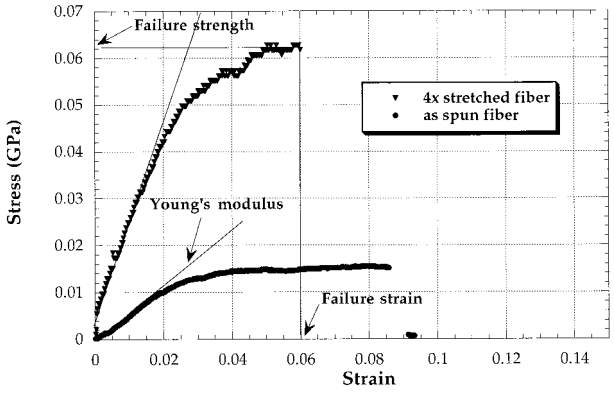

Figure 2. Stress–strain curves of polyaniline (EB) fibers.

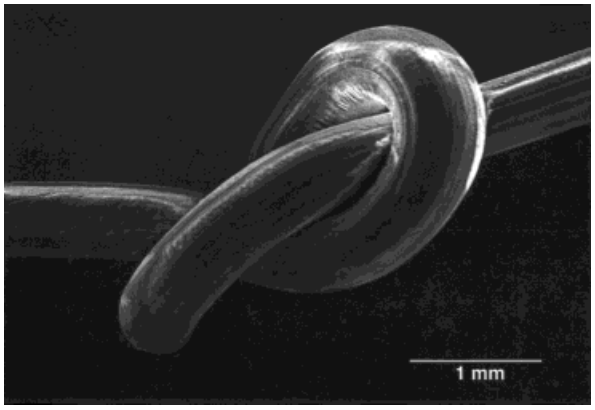

Figure 3. SEM micrograph of polyaniline EB fiber tied into a knot.

fiber. In contrast the 4-times stretched fiber breaks at a strain of 6%, which is about 30% smaller than the failure strain of as-spun fiber (9%). This difference in mechanical properties is in all likelihood due to the increased density and chain alignment in the 4-times stretched fiber. The measured densities of the as-spun and 4-times stretched fiber are 0.52 g/cm^3 and 0.92 g/cm^3, respectively. The above results suggest that the thermal stretching increases the Young's modulus, yielding strength and failure strength of the fiber.

Figure 3 shows a SEM micrograph of an as-spun fiber after it had been looped into a tight knot and qualitatively demonstrates that these HMW spun fibers can sustain large strain without failure. Although the fiber is strengthened by stretching, the simultaneous drop in failure strain makes these fibers more susceptible to breakage when forced into a tight a knot. The maximum achievable fiber draw ratio was strongly dependent on the residual solvent content and the specific temperature of the heated Cu rod. Extended drying resulted in lower NMP concentrations and tended to reduce the draw ratio. Too much residual solvent in the fiber in combination with excessively high temperatures of the copper rod resulted in overly rapid solvent evaporation and a pronounced disintegration of the fiber mophology.

Thermal Analysis of the EB Fiber

TGA studies of the HMW EB powder and fiber employed a heating rate of 5 °C/min while under constant nitrogen flux, and the resultant TGA thermograms are shown in Figure 4. The EB fiber was continuously washed with deionized water over a one-week period and then dried, under dynamic vacuum for 48 hours, prior to performing the thermogram. The resulting TGA curves for powder and fiber are essentially identical below 370 °C. This result suggests that the fiber is completely free of either NMP or 2 MA residues because both would have volatilized by this temperature and, also, the EB powder contains no NMP solvent. At higher temperatures, the EB fiber exhibits significant weight loss suggestive of decomposition. The EB fiber weight loss at 500 °C is ~ 49%, which is significantly higher than the 13% loss in the EB powder. We suspect that this may be due to the microporous nature of the fiber, which could provide for more rapid dissociation of decomposition products from the fiber. In addition (as discussed later) EB fiber is nearly 100% amorphous while the EB powder is partially crystalline. It is likely that the amorphous EB fiber is more susceptible to thermal decomposition as compared to the crystalline EB powder. A DSC thermogram for the EB fiber is shown in Figure 5 and there is a clear exothermic feature centered at 240 °C. Because this temperature is well below the temperature at which weight loss occurs in the EB fiber, we identify this feature as thermal crosslinking between the polymer in analogy to previous EB studies in which a similar DSC exotherm (at 220 °C for EB powder[19] and at 250 °C in EB film[16]) was attributed to crosslinking between the polymer chains.

Mechanical Properties of EB Dense Film

EB dense films were formed by thermal evaporation of the EB/NMP/2 MA solutions at ~ 120 °C

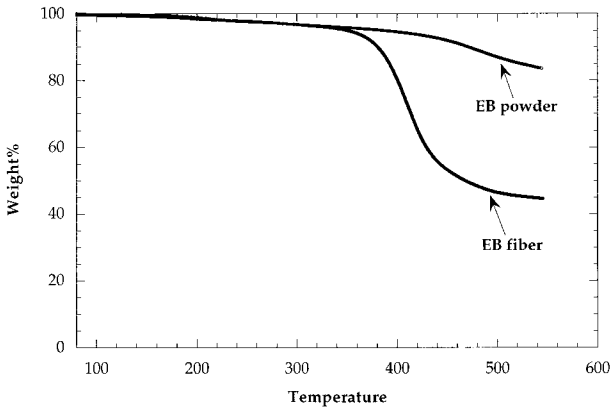

Figure 4. TGA scans of polyaniline EB powder and fiber.

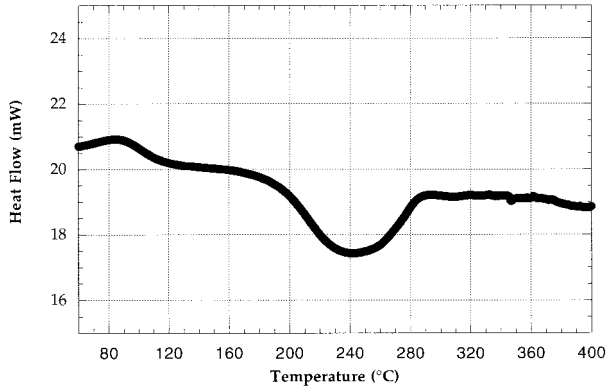

Figure 5. DSC scan of polyaniline EB fiber.

for 1 h. These dense films were later thermally stretched at draw ratios ranging from 2 to 4 times the original length. Figure 6 shows typical stress-strain curves for these films and clearly demonstrate a monotonic increase in Young's modulus with draw ratio. This trend is similar to results reported by Scherr et al.[5] The limiting Young's modulus for the unstretched film and the 4-times stretched film is 4.3 GPa and 14.0 GPa, respectively. Clearly the mechanical strength for both films and fibers is significantly improved by stretch orientation, which increases chain alignment at the molecular level. As was the case with oriented fibers, the failure strain at break systematically decreases with increased stretch. The yield strength also decreases with increasing stretch and indicates that these dense films become less tolerant of defect formation (they are embrittled). Because there is an enormous range of processing parameters both in preparing polymer solution and spinning fiber, it is likely that

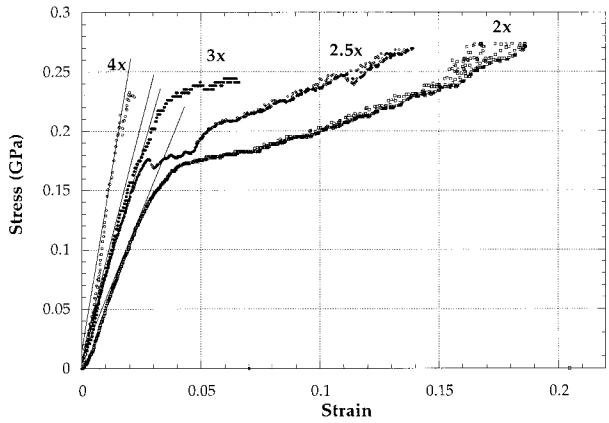

Figure 6. Stress–strain curves of polyaniline (EB) films with various stretching ratios.

Table I. Young's Modulus of the As-Spun Fiber from Three Different Spinneret Tips

Fiber Sample	Hole Dimension (μm)	Fiber Diameter (μm)	Young's Modulus (GPa)
#1	250	250	0.51
#2	500	480	0.41
#3	650	635	0.38

additional optimization will further improve the mechanical properties of EB fiber towards the theoretical limiting strength. At present, we assume that the measured mechanical properties of the stretched, dense film represent an upper-bound in the achievable strength of polyaniline EB fiber because the film exhibits the highest density among all articles prepared from these EB solutions.

Effect of the Spinneret Tips on the Mechanical Properties of the Fiber

In order to clarify the influence that fiber spinning has on the measured properties, a series of three spinneret tips with differing inner diameters of 650, 500, and 250 μm were tested. These fibers were extruded under identical conditions employing the same EB solution and water for the coagulation bath. The fibers were thoroughly rinsed, as described in the previous section, to ensure removal of solvent.

Results for the Young's modulus measurements are given in Table I. (Dimensions of the fibers were measured by using a optical microscope.) As seen from Table I, the spinneret tip with the smallest aperture produces fibers with the highest mechanical strength. This is most likely due to enhanced flow alignment of the polymer chains while in solution, as it passes through increasingly smaller spinneret tips. We note that the spinneret tips used in this study were not optimized. Additional work to determined the maximum fiber strength that can be achieved by modifying the configuration of the spinneret tip is planned.

Effect of Coagulation Bath and Heat Treatment on the Mechanical Properties of the EB Fiber

Controlling the choice of coagulation bath can be an important consideration. Termonia originally

proposed the addition of inorganic salt to a water coagulation bath in order to suppress macrovoid formation in membranes.[20] This resulting outcome is based on the claim that by changing the solvent/nonsolvent miscibility, one varies the exchange rate between solvent and nonsolvent. To test this approach, we replaced the coagulation bath water with a 1*M* LiCl aqueous solution. The tensile strength of as-spun fiber (0.66 GPa) from the 1*M* LiCl aqueous coagulation bath is higher as compared to that (0.51 GPa) for fibers processed in a pure water bath. This modest improvement is consistent with the proposed mechanism. Stretch orientation of these fibers, however, is more problematic. As-spun EB fiber, formed using 1*M* LiCl as coagulation bath and then immersed in 1*M* LiCl aqueous solution for 24 h, could only be drawn to 2 times the original length as compared with the 4-times drawn ratio for fibers using a pure water coagulation bath. As previously emphasized, a certain amount of residual NMP is required to lower the glass transition temperature to 110 °C, which is a necessary for improved thermal stretching of EB fibers. Angelopoulos et al. have shown that adding LiCl salt to EB and NMP solutions diminishes the tendency of EB to form aggregates (by reducing interchain H-bonding interactions) while in solution.[21] When fiber is immersed in 1*M* LiCl aqueous solution the LiCl has the ability to preferentially occupy the H-bonding sites bridging the NMP molecules and EB chains. Because the NMP is less tightly bound, this allows water to more effectively exchange with the residual NMP solvent still residing in the EB polymer chains. The final fiber obtained from this process contained very little NMP and hence has poorer draw properties. SEM micrographs of the fiber coagulated in 1*M* LiCl aqueous solution (not shown) are similar to the as-spun fiber processed using a water coagulation bath.

As was the case for fibers processed with water, these EB fibers can be converted into a partially crosslinked 3D network[5,22] by thermal treatment under inert atmosphere conditions. After heating the dried as-spun fiber at 250 °C under N_2 for 2 h, Table II shows that this fiber became significantly stronger than the untreated sample. The tensile strength of the 2-times stretched fiber is 1.02 GPa, which represents a 55% increase as compared to the as-spun fiber. In this instance the fiber was passed through a 250 μm spinneret tip into a 1*M* LiCl aqueous solution, maintained there for 24 h and then rinsed in a water tank for more than 6 days (with fresh water reintroduced every day to ensure removal of excess LiCl salt).

Conductivity of the Doped EB Fibers and Films

The conductivity data of fibers and films doped with various acids are given in Table III. All samples were immersed in acidic media for over 48 h to ensure complete doping. Thereafter, they were subjected to dynamic pumping for 72 h in order to remove the residual moisture. It is known that residual moisture can effect a significant increase in the emeraldine salt conductivity.[23,24] All the conductivity data reported in Table III were obtained from dried samples. Subsequent exposure to water vapor typically increases the fiber conductivity by almost an order of magnitude. For fibers with a 4-times draw ratio, the benzenephosphinic acid doped fiber exhibited the highest conductivity with a value of 10.3 S/cm. The fiber conductivity is lower in the cases of acetic acid and HCl doping. This is probably due to the fact that the fiber has a microporous structure and that both acids are volatile in nature, which may facilitate dedoping when placed under high vacuum. The stretched dense films always have higher conductivity than the stretched fibers presumably because of the nonporous structure of the dense film.

Chain alignment under uniaxial extension can occur and this process itself will be responsible for improvement of the conductivity in the drawn fibers and films. Unless there is appreciable bulk alignment by a significant minority of the polymer chains, X-ray scattering may not be the optimal structural probe. Infrared or optical dichroism would likely be more sensitive in this case. Still, we note that while the drawn fibers in this work have improved conductivities, they are not exceptional. The best polyaniline salts now have conductivities in excess of 1000 S/cm.

HCl-doped fiber was found to be more brittle than fibers doped with either acetic acid or benzenephosphinic acid. Similar results have been reported by Hsu et al.[13] They found that HCl and H_2SO_4 acids embrittle the poly(o-toluidine) fiber as a result of reduced cohesion force between polymer chains. In view of this tendency, inorganic acids should be viewed as poor candidates for fiber doping because they cause deterioration of the mechanical properties, and no benefit in the measured fiber conductivities.

As can be seen from the SEM pictures in Figure 7(a,b), the as-spun EB fiber shows numerous

Table II. Young's Modulus of the Fibers Processing under Different Conditions

Sample	#1	#2	#3	#4
Processing conditions	As-spun fiber (Coagulation bath is water)	As-spun fiber (Coagulation bath is 1*M* LiCl)	As-spun fiber (Coagulation bath is 1*M* LiCl) Heated at 250 °C for 2 h	2-times stretched fiber (Coagulation bath is 1*M* LiCl)
Young's modulus (relative strength) GPa	0.51	0.66	1.06	1.02

macrovoids, which compromise fiber strength, with a nominal 0.2–0.5 μm pore size. Future processing strategies must address the issues of macrovoid formation. Eliminating macrovoid formation and/or a reduction in the size of these micropores will densify the fiber structure and likely lead to further enhancement in the mechanical strength and conductivity equal to or better than that seen in the dense films.

Wide-Angle X-ray Diffraction (WAXD) of Polyaniline Powder and Fibers

Wide-angle X-ray diffraction (WAXD) data from the dedoped as-synthesized HMW EB powder, shown in Figure 8, contains a combination of both crystalline and amorphous components. The peak positions and intensity ratios are indicative of the crystalline ES-I polymorph.[25,26] It is important to note that fiber fabricated from concentrated solution without incorporation of GI has a small but finite percentage of crystallinity, which originates from the EB powder. With uniaxial extension there is a modest increase in the crystallinity as regions with partial nematic ordering undergo stress-induced crystallization. An integral component of this ordering/crystallization process is the existence of appreciable interchain hydrogen bonding in the starting materials.

In contrast, data from as-spun fiber fabricated from concentrated EB solution (with GI) exhibits essentially no crystallinity (see Fig. 8) and is comparable to data from dense EB cast films prepared in an analogous manner.[27] Even though this work employed highly concentrated solutions of EB, it is clear that the presence of GI antagonizes H-bonding interactions between the EB polymer chains and, as a result, effectively eliminates any tendency towards crystallization. The use of a GI (hydrogen bonding antagonist) in the preprocessing effectively eliminates this starting point and yields films and fibers with a distinctly different local interchain packing. Because the starting local interchain structure differs in our materials, there is no guarantee that drawing this fiber will produce any measurable crystallization.

Although drawing of these fibers does enhance chain alignment and improves the mechanical and electronic properties, it does not significantly increase the crystallinity in the fiber. WAXD data, with the diffraction vector in the perpendicular and parallel to the stretching direction, from the 4-times EB fiber are shown in Figure 9(a). The first amorphous halo, a broad peak centered

Table III. Conductivity of the Polyaniline EB Films and Fibers Doped in Various Aqueous Acid Solutions

Samples	Acid	Conductivity (S/cm)
4-times Stretched EB film	1*M* HCl	45
4-times Stretched fiber	1*M* HCl	3.4
Unstretched fiber	1*M* HCl	0.14
4-times Stretched EB film	1*M* CH_3COOH	0.7
4-times Stretched fiber	1*M* CH_3COOH	0.3
Unstretched fiber	1*M* CH_3COOH	6×10^{-4}
4-times Stretched EB film	Benzene phosphinic acid	40.6
4-times Stretched fiber	Benzene phosphinic acid	10.3
Unstretched fiber	Benzene phosphinic acid	0.1

about a 2ϑ angle of 19°, becomes somewhat more intense and sharper for the perpendicular direction. This same feature is weaker and less sharp in the parallel scattering profile. This suggests the development of slight changes in local interchain structure and a partial alignment of EB chains along the stretching direction, but the effect is modest. Higher draw ratios would be necessary for increased alignment. For low molecular weight fibers spun from concentrated NMP solutions lacking a gel inhibitor, previous work has shown that hot stretching can induce partial crystallization (up to 40%) with increasing draw ratio.[5,28] Clearly, addition of GI inhibits any tendency for the EB chains to crystallize. While this is desirable from a processing standpoint, it may ultimately limit the achievable fiber conductivity.

Figure 9(b) contains WAXD data from the 4-times stretched fiber doped with 1*M* HCl. The data is clearly different than that from the un-

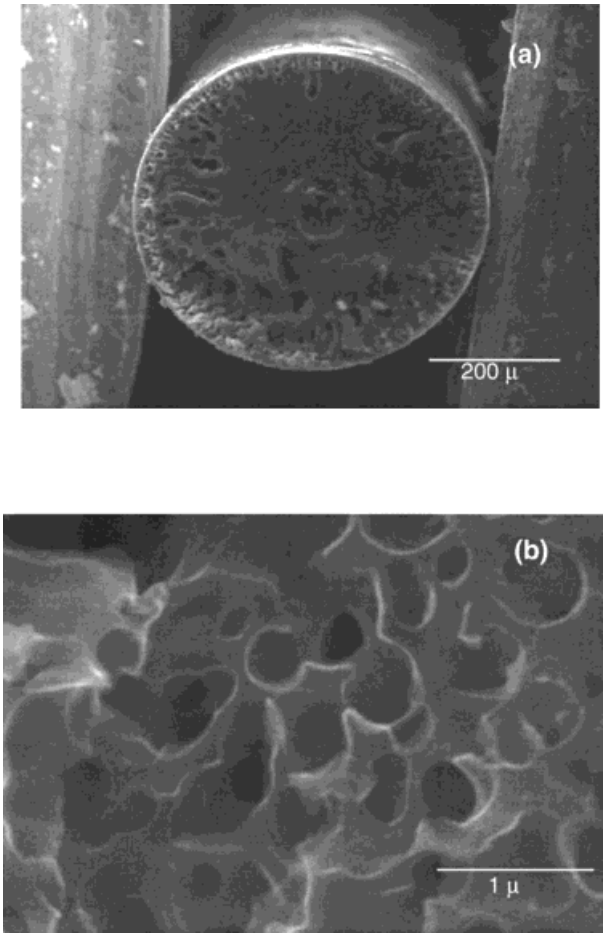

Figure 7. (a) SEM micrograph of cross section of a polyaniline EB fiber; (b) magnification of (a) near the center of the fiber.

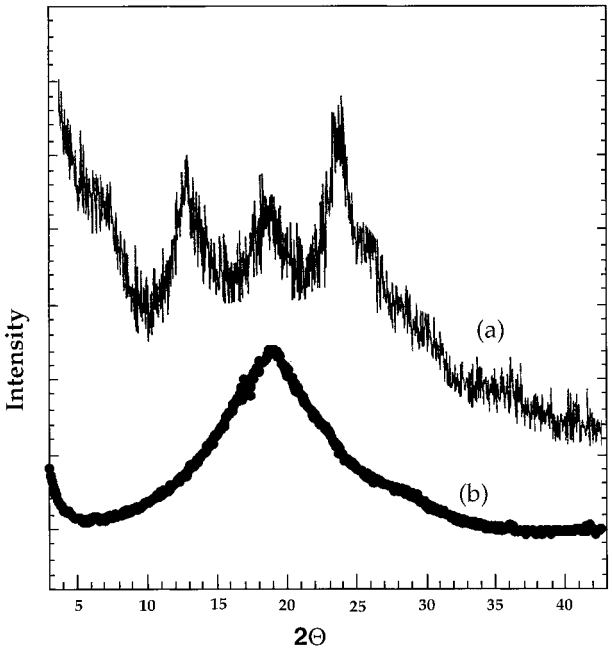

Figure 8. X-ray diffraction spectra of high molecular weight: (a) EB powder, (b) as-spun fiber.

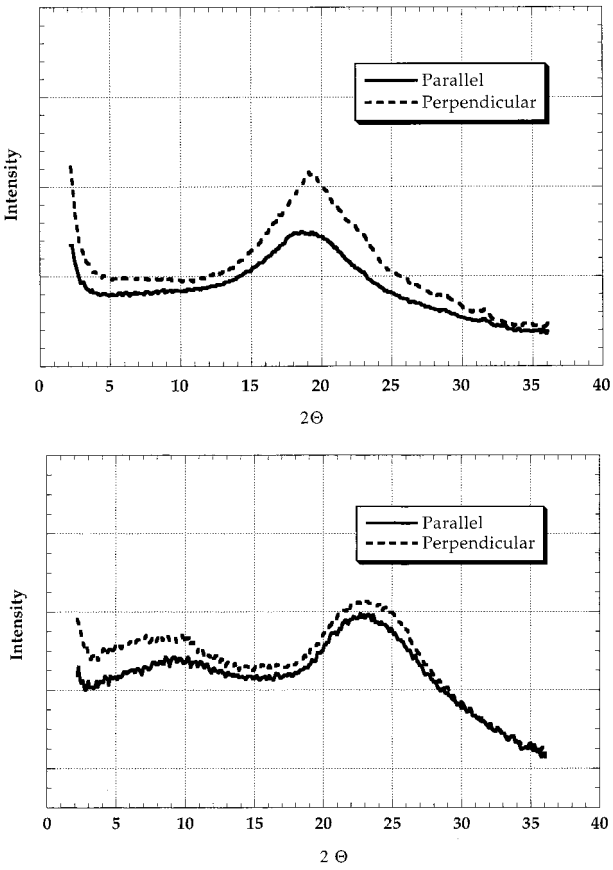

Figure 9. (a) X-ray diffraction spectra of 4-times stretched EB fiber; (b) X-ray diffraction of the 4-times stretched fiber doped in 1*M* HCl.

doped fiber but is comparable to amorphous film data for HCl doped polyaniline.[22] Because there is a new scattering feature centered about a 2ϑ angle of 9°, incorporating HCl within the polymer host has created inhomogeneities with a significantly larger length scale.

CONCLUSION

Processing of EB powder has been significantly enhanced by creating a stable, highly concentrated (>20% w/w), HMW polyaniline solution through the addition of a gel-inhibitor (2-methylaziridine) into the EB/NMP solution. This constituent appears to disrupt the interchain H-bonding interaction between the EB polymer chains, hence retarding gelation and crystallization. UV-Vis spectra of these concentrated solutions show no evidence of reduction of EB to the leucoemeraldine base form. Both the thermal stability and conductivity of the fiber are comparable with the EB powder suggesting no structural degradation at the molecular level. The mechanical strength of the fiber is further improved by chain alignment and cross-linking induced by hot-stretching. Reducing the spinneret tip diameter produces stronger fiber presumably due to better chain alignment, which occurs when EB solution is forced through a smaller aperture. These fibers remain amorphous even after being stretched at up to 4 : 1 draw ratios. Still the mechanical properties of the stretched dense films are better and the measured conductivities remain higher than those of stretched fiber because of macrovoid formation and lower overall material density. Doping the fiber with inorganic acid (HCl) embrittles the fiber, whereas doping with organic acid (acetic acid, benzenephosphinic acid) does not appreciably affect the mechanical strength. Continued improvements in the processing and post-treatment of fiber are likely to yield even further advancement in the fiber properties.

This work is primarily supported by the Laboratory Directed Research and Development program through the Industrial Partnership Office of Los Alamos National Laboratory. Partial support of this work (M.J.W.) through NSF grant DMR-9631575 is gratefully acknowledged.

REFERENCES AND NOTES

1. Wang, H. L.; MacDiarmid, A. G.; Epstein, A. J. Synth Met 1996, 78, 33.
2. Takashima, W.; Kancko, M.; Kaneto, K.; MacDiarmid, A. G. Synth Met 1995, 71, 2265.
3. Wang, H. L.; Mattes, B. R. Synth Met 1999, 102, 1333.
4. Oh, E. J.; Min, Y.; Wiesinger, J. M.; Manohar, S. K.; Scherr, E. M.; Prest, P. J.; MacDiarmid, A. G.; Epstein, A. J. Synth Met 1993, 977, 55–57.
5. Sherr, E. M.; MacDiarmid, A. G.; Manohar, S. K.; Master, J. G.; Sun, J. G.; Tang, Y. X.; Druy, M. A.; Glatkowski, P. J.; Cajipe, V. B.; Fisher, J. E.; Cromack, K. R.; Jozefowitz, M. E.; Ginder, J. M.; Macall, R. P.; Epstein, A. J. Synth Met 1991, 735, 41–43.
6. MacDiarmid, A. G.; Manohar, S. K.; Scherr, E. M.; Tang, X.; Druy, M. A.; Glatkowski, P. J.; Epstein, A. J. Polym Mater Sci Eng 1991, 64, 254.
7. Cohen, J. D.; Tietz, R. F. U. S. Patent 5,135,682, Aug. 4, 1992.
8. Hsu, C. H.; Cohen, J. D.; Tietz, R. F. Synth Met 1993, 59, 37.
9. Han, C. C.; Jeng, R. C. Chem Commun 1997, v 6, 553.
10. (a) Chaco, A. P.; Hardaker, S. S.; Huang, B.; Gregory, R. V. Proceeding of Material Research Society,

Boston, Fall 1995; (b) Rajiv, J.; Gregory, R. V. Synth Met 1995, 74, 263.
11. Eaiprasersak, K.; Gregory, R. V. Antech '98 1998, 2, 1263.
12. Andreatta, A.; Heeger, A. J.; Smith, P. Polym Commun 1990, 31, 275.
13. Hsu, C. H.; Epstein, A. J. Synth Met 1997, 84, 51.
14. Matttes, B. R.; Wang, H. L.; Yang, D.; Zhu, Y. T.; Blumenthal, W. R.; Hundley, M. Synth Met 1997, 84, 45.
15. Angelopoulos, M.; Asturias, G. E.; Ermer, S. P.; Ray, A.; Scherr, E. M.; MacDiarmid, A. G. Mol Cryst Liq Cryst 1988, 160, 151.
16. Wei, Y.; Jang, G. W.; Hsueh, K. F.; Scherr, E. M.; MacDiarmid, A. G.; Epstein, A. Polym J 1992, 33, 314.
17. Lee, H. T.; Chung, K. R.; Cheng, S. A.; Wei, P. K.; Hsu, J. H.; Fan, W. Macromolecules 1995, 28, 7645.
18. Matttes, B. R.; Wang, H. L.; Yang, D. ANTEC Proceeding of the SPE 55th Annual Technical Conference, 1997, p 1463.
19. Wang, X. H.; Geng, Y. H.; Wang, L. X.; Jing, X. B.; Wang, F. S. Synth Met 1995, 69, 263.
20. Termonia, Y. J Membr Sci 1995, 104, 173.
21. Angelopoulos, M.; Liao, Y. H.; Furman, B.; Graham, T. Macromolecules 1996, 29, 3406.
22. MacDiarmid, A. G.; Epstein, A. J. Lower-Dimensional Systems and Molecular Electronics; Metzger, R. M. et al., Eds.; Plenum Press: New York, 1991.
23. Angelopoulos, M.; Ray, A.; MacDiarmid, A. G.; Epstein, A. J. Synth Met 1987, 21, 21.
24. Javadi, H. H. S.; Angelopoulos, M.; MacDiarmid, A. G.; Epstein, A. J. Synth Met 1988, 26, 1.
25. Pouget, J. P.; Jozefowicz, M. E.; Epstein, A. J.; Tang, X.; MacDiarmid, A. G. Macromolecules 1991, 24, 779.
26. Winokur, M. J.; Mattes, B. R. Macromolecules 1998, 31, 8183.
27. Maron, J.; Winokur, M. J.; Mattes, B. R. Macromolecules 1995, 28, 4475.
28. Fischer, J. E.; Zhu, Q.; Tang, X.; Scherr, E. M.; MacDiarmid, A. G.; Cajipe, V. G. Macromolecules 1994, 27, 5094.